ATTENUATION OF SURFACE ACOUSTIC WAVES BY SPIN–WAVE EXCITATIONS IN $Co_{60}Fe_{20}B_{20}$

K. M. SEEMANN[*,‖], F. KRONAST[†], A. HÖRNER[‡], S. VALENCIA[†], A. WIXFORTH[‡], A. V. CHAPLIK[§] and P. FISCHER[¶]

[*]*Physik Department E21 & Heinz Maier-Leibnitz Zentrum (MLZ)*
Technische Universität München, Germany

[†]*Helmholtz-Zentrum Berlin für Materialien und Energie*
Albert-Einstein-Strasse 15, Berlin, Germany

[‡]*Institut für Physik, Experimentalphysik I*
Universität Augsburg, Germany

[§]*Institute of Semiconductor Physics*
Russian Academy of Sciences
Novosibirsk, Russia

[¶]*Center for X-ray Optics*
Lawrence Berkeley National Laboratory
Berkeley, California 94720, USA
[‖]*klaus.seemann@frm2.tum.de*

The acousto-magnetic attenuation of surface acoustic waves (SAW) in an $Co_{60}Fe_{20}B_{20}$ exchange spring magnet is evidenced experimentally. By high-resolution magnetic imaging using photo-excitation electron microscopy (XPEEM) and magnetometry measurements, the deflection of the ferromagnet from its equilibrium state is visualized. Along a harmonic oscillator model with damping term, the experimental observation of SAW attenuation is attributed to low-frequency spin wave generation in a magnetic exchange spring. Measuring the SAW attenuation at four eigenfrequencies generated via on-chip higher-harmonic generation, we obtain a sub-GHz resonance at $f_0 = 538\,\mathrm{MHz}$.

Keywords: Spin waves; exchange bias; CoFeB; magnetic ripple domains; surface acoustic waves; SAW; photo-excitation electron microscopy; XPEEM.

[‖]Corresponding author.

1. Introduction

Understanding and utilizing spin-accumulation effects[1] and spin-pumping mechanisms[2] are important and fundamental steps forward to meet future technological requirements towards novel low-energy consumption electronics. In that sense, an alternative methodical approach is surface acoustic waves (SAW), which could play an important role for new spin-transport devices on the basis of magneto-elastic effects analogous to ultrafast magnetization dynamics in applying short and intense laser pulses to exchange-biased ferromagnetic systems. The presented experimental results may prove useful for the probing and excitation of other noncollinear magnetic structures with surface acoustic waves towards novel, low energy-consumption spintronic devices.

In this work, we describe the experimental SAW amplitude attenuation in exchange-biased $Co_{60}Fe_{20}B_{20}$ upon deflection of the magnetization from the equilibrium state towards an exchange spring magnet by on-chip higher-harmonic generation and relate the observations to results obtained from high-resolution photoelectron microscopy performed at a synchrotron light source. Direct evidence is delivered by the SAW amplitude damping ΔS_{21}, the two-gate high-frequency forward transmission parameter $\Delta S_{21} = \frac{b_2}{a_1}$,[3] where b_2 denotes the wave emitted from gate 2 and a_1 represents the incoming wave at gate 1. Our SAW attenuation experiments are accompanied by magnetic XPEEM imaging of the rotational deflection of an exchange spring.

2. Experimental Methods

An exchange-biased $Co_{60}Fe_{20}B_{20}$ layer of 20 nm thickness was prepared on an iridum-manganese $Ir_{20}Mn_{80}$ underlayer. This bi-layer was deposited by H-field assisted magnetron-sputtering at room temperature onto a epitaxy-ready polished and degassed single-crystal lithium niobate substrate with a special rot.-128°-cut that offers the capability of piezo-electrically launched Rayleigh-type surface acoustic waves. In detail, a tantalum base layer of 2 nm thickness was followed by 5 nm $Ni_{20}Fe_{80}$ and 20 nm of anti-ferromagnetic $Ir_{20}Mn_{80}$, thus yielding an exchange-bias of $\mu H_{\text{Exchange-Bias}}$=3.6 mT for a 20 nm thick $Co_{60}Fe_{20}B_{20}$ ferromagnet deposited on top. More details on the magnetic properties of this system can be found in Seemann *et al.*[4] For launching surface acoustic waves, interdigitated SAW transducers were deposited directly onto the lithium niobate substrates by evaporating 5 nm of titanium and 20 nm of gold employing optical lithography and a subsequent lift-off technique. The lithographically patterned fundamental SAW wavelength was 30 microns, corresponding to an eigenfrequency of $f_0 = 112$ MHz.

2.1. *Magnetic Imaging*

Magnetic imaging of the CoFeB layer was performed by photoemission electron microscopy XPEEM, exploiting the element specific X-ray magnetic circular dichroism (XMCD) effect at the L3 resonance of Cobalt at 778 eV, as schematically shown in Fig. 1(a). An angular deflection of ±10° from the direction of the exchange bias field was determined in the magnetic equilibrium state.

2.2. *SAW Attenuation*

The SAW amplitude attenuation was measured at four frequencies generated by higher-harmonic generation. The on-chip harmonic generation allows for four different probe frequencies, $f_{\text{SAW}} = 112$ MHz, 336 MHz, 560 MHz and $f_{\text{SAW}} = 784$ MHz, respectively, as shown for a magnetic field applied perpendicular to the exchange bias field in Fig. 1(b). The experimental data for the attenuation parameter is plotted with an offset for clarity.

The magnetic contrast displayed in Fig. 1(c) represents the magnetization component pointing along the incidence direction of the X-ray beam. The sample was mounted on a special sample holder[5] that allows for magnetic in-plane fields applied to the sample up to 50 mT during imaging. At remanence, we observe magnetic ripple domains, which most likely originate from magnetic frustration at the ferromagnetic–antiferromagnetic interface.[6] With increasing field perpendicular to the exchange-bias direction the ripple domains are removed, while the magnetization rotates into the field direction. The stripe-shaped magnetic domain ripples visualize the rotation of the CoFeB ferromagnet, depicted also by the encircled symbol in the lower left corner of the magnetic images representing the alignment of the total magnetization.

3. Results and Discussion

The transmission properties of the SAW are recorded in terms of attenuated amplitude ΔS_{21} representing

the real part in the Gaussian system. The maximal attenuation of the surface acoustic waves due to the rotational deflection of the CoFeB magnetization from its equilibrium state upon applying a magnetic field perpendicular to the exchange bias direction is observed at a frequency of $f_{SAW} = 560\,\text{MHz}$ [Fig. 1(a)]. While the attenuation shows its largest negative value of $\Delta S_{21} = -0.25\,\text{dB}$ at the fifth harmonic $f_{SAW} = 560\,\text{MHz}$, the attenuation remains below a value of $\Delta S_{21} = -0.1\,\text{dB}$ for the first, third and seventh harmonic frequency.

Therefore, employing the frequency of the fifth higher-harmonic for SAW attenuation measurements is considered preferable due to the pronounced sensitivity and signal-to-noise ratio. Our experimental technique to assess the SAW attenuation within the CoFeB thin film is based on a pulsed-source Fourier transform measurement. The Kramers–Kronig relations lead to an expression for the SAW velocity dependent on the attenuation of the SAW based on sub-GHz spin-wave excitations within the noncollinear rotational twist of the CoFeB magnetization. The acousto-magnetic attenuation obtained experimentally from the SAW transmission parameter S_{21} and consequently-based on the Kramers–Kronig relations[3] — the phase

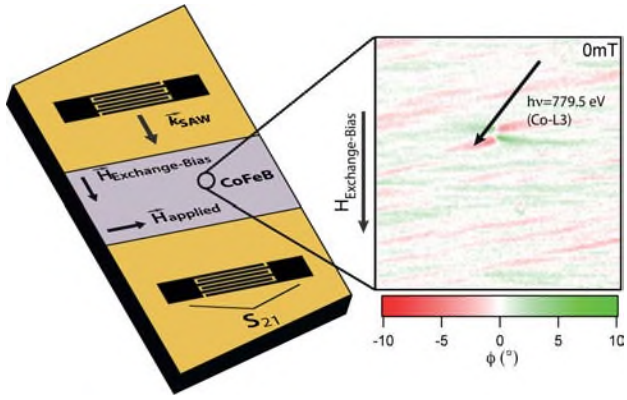

(a)

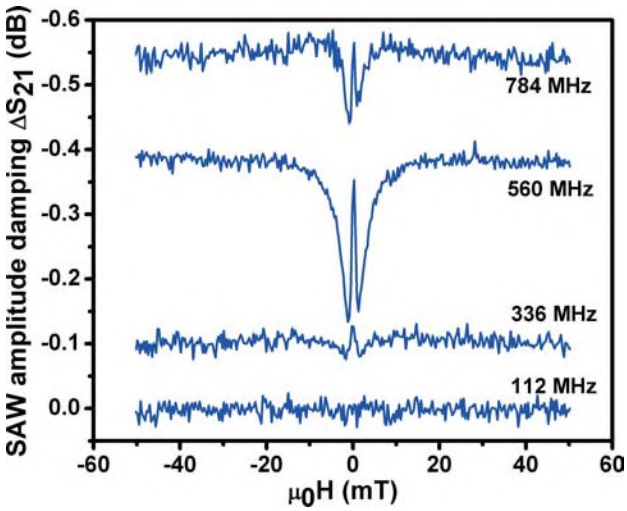

(b)

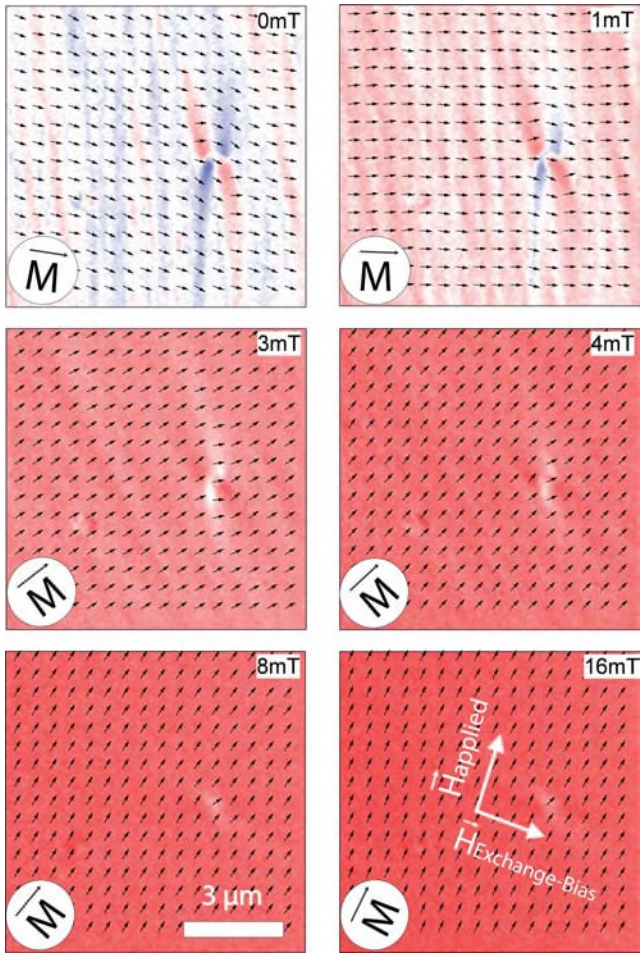

(c)

Fig. 1. Schematic of the surface acoustic wave attenuation experiment and the magnetic imaging by XPEEM (a). The amplitude damping ΔS_{21} of the surface acoustic waves after transmission through the $Co_{60}Fe_{20}B_{20}$ ferromagnet (b) detected as a function of magnetic field applied in-plane and perpendicular to the direction of the exchange bias field. By on-chip higher-harmonic generation the deflection of the exchange spring magnet was probed by four frequencies. A maximal SAW amplitude attenuation was observed for $f_{SAW} = 560\,\text{MHz}$. Magnetic ripple domains recorded by XPEEM reveal the correlation of the acousto-magnetic attenuation and the rotating ferromagnet forming an exchange-spring structure (c). The perpendicular orientation of applied field and exchange bias field is displayed in the XPEEM image taken at 16 mT, the arrows represent the direction of the local magnetization and the encircled M in the lower left corner illustrates the orientation of the total magnetization at the field value given (color online).

velocity c at which the SAWs are propagating through a thin film of magnetic material is a function of the magnetic domain state,[7]

$$\Delta c = c(\omega) - c_0 = \frac{2c_0^2}{\pi} \int_{\omega_0}^{\omega} \frac{|S_{21}(\omega')|}{\omega'^2} d\omega'. \quad (1)$$

The attenuation of SAW in the exchange-biased CoFeB exchange spring magnet originates from a decreased SAW phase velocity, which is caused by spin–wave excitations akin to an harmonic oscillator with damping term. The equation of motion for an infinitesimally small deviation $\Delta \mathrm{d}_{SAW}$ of the magnetic moment $\mathbf{m}$ from its field dependent equilibrium position M_0 of the exchange spring structure is given by

$$\dot{m} = g\alpha_{ik}\left[\frac{\partial^2 \mathbf{m}}{\partial x_i \partial x_k}\right], \quad (2)$$

wherein g denotes the gyromagnetic ratio and α represents the tensor of materials parameters, see Ref. 8.

The characteristics of the magnetic field-dependent SAW amplitude attenuation as displayed in Fig. 1(b) can be separated into two effects occurring consecutively one after another. Starting at zero magnetic field, the $\Delta \mathrm{S}_{21}$ for the equilibrium state of the magnetic ripple domains exhibits a high transmissivity for the 560 MHz SAW and consequently a low relative amplitude attenuation corresponding to a high relative SAW phase velocity, cf. Eq. (1). The dissipation of the SAW power by spin–wave excitation is therefore low. This changes dramatically by applying a magnetic field perpendicular and in-plane to the exchange bias direction. At an applied magnetic field of 1 mT the $\Delta \mathrm{S}_{21}$ attenuation parameter reaches a global minimum representing also a global minimum of the SAW phase velocity and a maximum in deposited SAW power. This pronounced effect is attributed to the gradual alignment of spins within the magnetic ripple domains enabling an considerably enhanced efficiency in spin–wave emission at 1 mT applied magnetic field. The reduced magnetic long-range order along k_{SAW} in comparison to the SAW wavelength of approximately 7 μm in the equilibrium state at zero field therefore has low susceptibility to SAW-induced spin wave emission. Increasing the magnetic domain size along k_{SAW} and removing the magnetic domains changes the CoFeB ferromagnet to the high-susceptibility state of SAW power dissipation by spin wave excitations. Surpassing the magnetic field threshold necessary to deflect the CoFeB layer rotationally from the pinned direction parallel to the exchange bias direction gradually reduces the SAW power dissipation by sub-GHz spin waves which saturates at 16 mT corresponding to the magnetic saturation observed by XPEEM. The increased magnetic stiffness of the CoFeB ferromagnet in zero applied field comparable to the magnetic stiffness upon saturation is attributed to frustrated spins originating at the ferromagnetic–antiferromagnetic interface as described in Ref. 6. Our experimental results indicate good qualitative agreement with recent theoretical predictions by Saeki on the basis of time-convolutionless equations with external driving terms expressed by thermo-field dynamics (TFD), i.e., the TCLE method.[9,10] This theory has its origin in quantum field theory and enables investigations of the linear response of a many-body system interacting with its environment such as a heat reservoir, phonon or magnon reservoir. Considering a ferromagnetic spin system with uniaxial anisotropy that is interacting with a phonon reservoir and with an external magnetic driving field, a transverse magnetic susceptibility is derived analytically and examined numerically. The results of the TCLE theory predict increased peak heights of the line shapes in the resonance region near zero field for low frequencies, a phenomenon that we have observed experimentally in our SAW attenuation experiments in the sub-GHz frequency regime. The TCLE theory also confirms within the damped oscillator model decreasing peak heights in combination with motional broadening of the line shapes for increasing characteristic frequency of the phonon reservoir. Large magnitudes of spin according to the TCLE method lead to enhanced peak heights for low frequencies and decreased peak heights for high frequencies, both of which is the case in our experimental observations upon increasing the experimental magnetic field applied perpendicular to the exchange bias field of the CoFeB thin film [Fig. 1(b)].

4. Conclusion

In conclusion, based on the Kramers–Kronig relations we attribute the experimentally observed SAW attenuation to a decreased phase velocity of the surface acoustic waves driven through the

CoFeB due to sub-GHz spin-wave excitations. Using synchrotron light monochromatized to the Co-L3 edge in combination with high-resolution XPEEM we have imaged magnetic ripple domains as a consequence of a strong exchange bias field acting on a thin film of CoFeB. The stripe-shaped ripple domains allow us to visualize the deflection of the magnetization upon applying a magnetic field in-plane and perpendicular to the direction of the exchange bias field, thus generating an exchange spring, i.e., a noncollinear rotational twist within the ferromagnet which is pinned at the interface to the iridium-manganese anti-ferromagnet. The SAW experiments were performed at four eigen–frequencies generated by on-chip higher-harmonic generation and yield a sub-GHz spin wave resonance at $f_0 = 538\,\mathrm{MHz}$. Our experimental results verify in large parts the predictions of quantum field theory (TCLE method) for transverse susceptibilities of ferromagnetic spin wave interaction with phonon and magnon reservoirs.

Acknowledgments

P. F. acknowledges support by the U.S. Department of Energy (DE-AC02-05-CH11231). K.M.S acknowledges the Helmholtz-Zentrum für Materialien und Energie, Berlin for beamtime. K. M. S., A. H. and A. W. thank the Nanosystems Initiative Munich (NIM) for support.

References

1. C. M. Jaworski *et al.*, *Phys. Rev. Lett.* **106**, 186601 (2011).
2. E. Shikoh *et al.*, *Phys. Rev. Lett.* **110**, 127201 (2013).
3. M. O'Donnell, E. T. Jaynes and J. G. Miller, *J. Acoust. Soc. Am.* **69**, 696 (1981).
4. K. M. Seemann *et al.*, *Phys. Rev. Lett.* **107**, 866031 (2011).
5. F. Kronast *et al.*, *Surf. Interface Anal.* **42**, 1532 (2010).
6. E. Jiménez *et al.*, *Phys. Rev. B* **80**, 014415 (2009).
7. R. C. OHandley, Modern Magnetic Materials: Principles and Applications (John Wiley & Sons, 2000), p. 240.
8. E. M. Lifshitz and L. P. Pitaevskyi, *Statistical Physics: Theory of the Condensed State (Course of Theoretical Physics)*, Vol. IX (Butterworth-Heinemann, 1980).
9. M. Saeki, *Progr. Theor Phys.* **121**, 165 (2009).
10. M. Saeki, *Physica A.* **390**, 1884 (2011).